Conf-910435--72

UCRL-JC-104931
PREPRINT

Spent Fuel Waste Form Characteristics: Grain and Fragment Size Statistical Dependence for Dissolution Response

R. B. Stout
H. Leider
H. Weed
S. Nguyen
W. McKenzie
S. Prussin
C. N. Wilson
W. J. Gray

THIS PAPER WAS PREPARED FOR SUBMITTAL TO
The Second Annual International High Level Radioactive Waste Management Conference & Exposition, April 28-May 3, 1991
at Caesars Palace, Las Vegas, NV

Manuscript Date: December 1990
Publication Date: April 1991

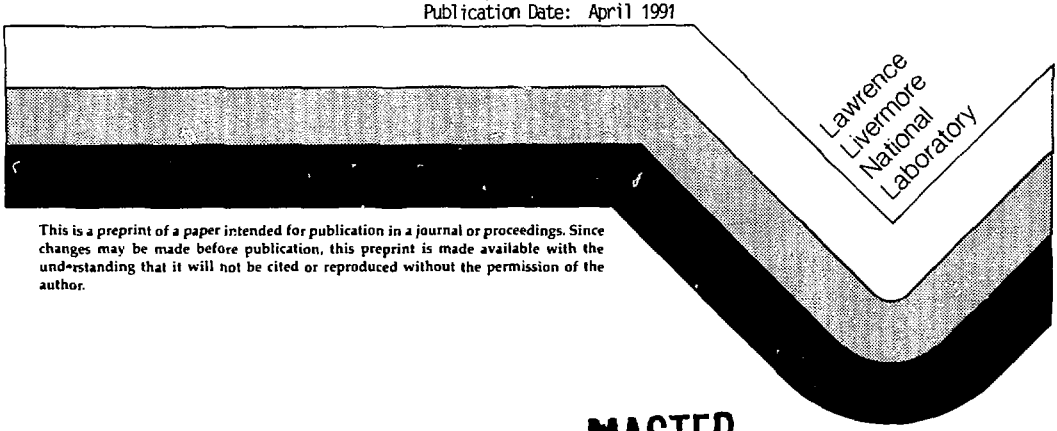

UCRL-JC--104931

DE91 012027

Spent Fuel Waste Form Characteristics: Grain and Fragment Size Statistical Dependence for Dissolution Response

R. B. Stout, H. Leider, H. Weed
S. Nguyen, W. McKenzie, S. Prussin
University of California/LLNL
P.O. Box 808, L-201
Livermore, CA 94550
(415) 422-3965

C. N. Wilson, W. J. Gray
Battelle/PNL
P.O. Box 999
Richland, WA 99352
(509) 376-3453

ABSTRACT

The Yucca Mountain Project of the U.S. Department of Energy is investigating the suitability of the unsaturated zone at Yucca Mountain, NV, for a high-level nuclear waste repository. All of the nuclear waste will be enclosed in a container package. Most of the nuclear waste will be in the form of fractured UO_2 spent fuel pellets in Zircaloy-clad rods from electric power reactors. If failure of both the container and its enclosed clad rods occurs, then the fragments of the fractured UO_2 spent fuel will be exposed to their surroundings. Even though the surroundings are an unsaturated zone, a possibility of water transport exists, and consequently, UO_2 spent fuel dissolution may occur. A repository requirement imposes a limit on the nuclide release per year during a 10,000 year period; thus the short term dissolution response from fragmented fuel pellet surfaces in any given year must be understood. This requirement necessitates that both experimental and

analytical activities be directed toward predicting the relatively short term dissolution response of UO_2 spent fuel. The short term dissolution response involves gap nuclides, grain boundary nuclides, and grain volume nuclides. Analytical expressions are developed that describe the combined geometrical influences of grain boundary nuclides and grain volume nuclides on the dissolution rate of spent fuel.

INTRODUCTION

The initial release rate observed for some highly soluble radionuclides in UO_2 spent fuel leaching tests can be several orders of magnitude greater than the release rate that occurs a half a year later [1,2,3]. This has been termed "rapid release" and it has contributions from the inventories of the dissolving radionuclides on the fragment surfaces of broken spent fuel pellets and from the dissolving radionuclides in the subset of grain boundaries contiguous to the fragment surfaces. Thus, in terms of geometrical characteristics of spent fuel, the surface area of pellet fragments and the number of grain boundaries intersecting a fragment surface area are both important physical quantities in an analytical representation for release rate.

In order to begin quantitating these available but limited experimental observations, and more importantly, to provide a basis for additional experimental planning, a preliminary dissolution response model is being developed that depends explicitly on statistical density measures of fragment geometry and grain boundary/volume geometries. The statistical concepts of the model arise physically because spent fuel fragments and their associated grain boundary attributes have a random or stochastic geometrical character when considering the available spent fuel for a repository.

The model is derived by first considering an arbitrary set of fragments. The volume of each fragment is decomposed into spatial domains that are approximated by pyramidal

subvolumes, with their apex at the center of the fragment. This spatial decomposition describes the set of fragments in terms of the number of pyramidal subvolumes per unit size class, which is a probabilistic density function. Within each pyramidal subvolume, a number density for the grain boundary/volume size classes can also be described in terms of probabilistic concepts. In fact, the analytical representation for the number density of a grain boundary/volume distribution is also a probabilistic density function that was discussed previously [4]. This approach was initially developed to describe deformations statistically for particles of granular materials [5].

Using the density functions for fragments and for grain boundary/volumes, an expression can be written for the expected values of exposed grain volume surfaces and their associated radionuclide inventories being dissolved at a grain volume dissolution rate. Also, an expression can be written for the expected value of exposed grain boundary surfaces (here it is assumed that a grain boundary has a small but finite leaching width) and their associated radionuclide inventories being dissolved at a grain boundary dissolution rate. For an arbitrary sample of spent fuel fragments, and neglecting the cladding gap dissolution response, the sum of these two expressions is the fragment dissolution rate. As discussed in the next section this dissolution rate has an explicit statistical dependence on the grain boundary/volume size distribution and on the fragment size distribution of the sample.

GRAIN AND FRAGMENT STATISTICS FOR DISSOLUTION RATE

The rate of dissolution of a body depends on two vector functionals; one describes the local removal rate of material per unit area per unit time at points on the surface of the

body and the other functional describes the surface area evolution as the body decreases in size due to dissolution. The objective here is to develop a preliminary model for the functional describing the surface area evolution. For spent fuel, this depends on grain and fragment geometries. In the case of a body, or a set of uniformily shaped bodies, with a simple geometry (sphere, cylinder, block, etc.) that dissolves with a constant and spatially uniform removal rate, the problem of analytically representing the dependence on surface area evolution is tractable in an exact, deterministic sense. This follows because the initial geometrical shape is easily represented analytically; and this shape remains time invariant (i.e., a sphere remains spherical) as the shape decreases in size due to dissolution.

However, in the case of spent fuel fragments, the set of bodies (fragments) are not initially of a simple geometrical shape and they also have a domain of sizes. In addition, there may also be a domain of material removal rates that may not be spatially uniform; particularly for fragment surface areas that have exposed grain boundary dissolution and grain volume dissolution simultaneously. Thus, for spent fuel, fragment surfaces, and their exposed grain boundary area and grain volume area, are appropriately described in a stochastic or probabilistic sense. Hence, a model for spent fuel dissolution rate would not be classical deterministic with respect to surface area measures. Nevertheless, expected values and conservative dissolution rate estimates can be calculated on the basis of statistical measures of the fragments, the grain boundaries, and the grain volumes that are contained in a unit spatial volume, e.g., a fuel rod. To simplify the concepts of a stochastic dissolution model that incorporates statistical measures, only fragment statistics are considered first; and grain boundary and grain volume influences are addressed later.

To develop these fragment statistics, consider a single fragment as illustrated in Figure 1; but to begin the development, assume the zone of dissolution has zero thickness. The surface geometry can be approximated by a finite set of exterior surface planes that

enclose the fragments' volume. An example of a plane (base of the triangle) is illustrated in Figure 1; and its position is shown after a time interval of dissolution has occurred. The areal size of any surface plane can be represented by choosing two orthogonal vectors in the plane, say $\underline{p}$ and $\underline{q}$, whose dimensions are such that their cross product is a perpendicular vector directed inwardly to the fragment, and its magnitude is the area of the plane. Each of the planes is a base for a pyramidal subvolume of the fragment. The height of this pyramidal subvolume is a perpendicular vector from the base plane to the center of the fragment. This height vector will be denoted as $\underline{h}$, note that it is parallel to the cross product vector ($\underline{p} \times \underline{q}$) which can be written with Cartesian tensor notation as $e_{ijk}\, p_j q_k$ where e_{ijk} is the alternating tensor. This method of selecting a set of approximating exterior planes to represent a fragment's surface, each with their vector attributes, $\underline{p}$ and $\underline{q}$, along with their associated height vector $\underline{h}$ forms a spatial subdivision of a fragment into pyramidal subvolumes. Furthermore, each fragment in a set of fragments can be subdivided; thus, a large number of pyramids with their associated vector attributes ($\underline{p}$, $\underline{q}$, $\underline{h}$) can be identified. Given these vectors to describe a pyramid, recall that the volume of a pyramid is written in Cartesian tensor notation as $h_i e_{ijk}\, p_j q_k/3$.

As viewed from the pyramidal volumes, it is this volume that is being dissolved at a material removal rate; however, the only exposed surface would be planes parallel to the ($\underline{p} \times \underline{q}$) plane for the case of spatially homogeneous removal rate for a pyramid subvolume. Then, assuming that the material removal rate is spatially homogeneous for a fragment, a pyramid from a fragment dissolves one-dimensionally along its height vector attribute $\underline{h}$. The removal rate along vector $\underline{h}$ can be represented as a velocity, $\dot{H}_V \underline{h}$, where $\dot{H}_V$ has dimensions per unit time and the velocity has length units of vector $\underline{h}$. If the dissolution began at time t=0, then at some later time $t=\tau$, the dissolution front has progressed along vector $\underline{h}$ to a position represented by $H_V \underline{h}$ where H_V is the integral of $\dot{H}_V$ over the time interval (t=0 to $t=\tau$) with $H_V=0$ at t=0. At this later time, the surface area at the dissolution

front has been reduced from ($\underline{p}$ x $\underline{q}$) initially; because the magnitudes of vector attributes $\underline{p}$ and $\underline{q}$ are each reduced by the factor (1-H_V). Thus, at time $t = \tau$, the ($\underline{p}$ x $\underline{q}$) area becomes in Cartesian tensor notation $e_{ijk}\, p_j q_k\, (1\text{-}H_V)^2$. Using this area and the removal rate, the volume rate of material removed at time τ is $\dot{H}_V\, h_i\, e_{ijk}\, p_j q_k\, (1\text{-}H_V)^2$ per pyramid. The species dissolution rate, for the different radionuclide species, can be represented in terms of their inventory per unit volume times the volume dissolution rate. Thus, denoting the inventory per unit volume as I_{VK} for the "K^{th}" radionuclide species, and assuming that it is uniform within a fragment (recall that the grain boundary and grain volume influence will be added later), then the dissolution rate for a single pyramid with attributes ($\underline{p}$, $\underline{q}$, $\underline{h}$, H_V, $\dot{H}_V$) at time τ is

$$\dot{D}_{VK}(\tau) = I_{VK}\, h_i\, e_{ijk}\, p_j q_k\, (1\text{-}H_V)^2\, \dot{H}_V \qquad (1)$$

Now, the summation of the dissolutions from a set of pyramids defined from a set of fragments can be obtained by "counting" the number of pyramids at each attribute value ($\underline{p}$, $\underline{q}$, $\underline{h}$, H_V, $\dot{H}_V$). Here, the mathematical assumption is made that the number of fragments in a unit volume is large and that the even larger number of pyramidal subvolumes from dividing the fragment volumes would be countable and regular within a neighborhood of each value of the vector attribute domain; this amounts to assuming that a probabilistic density function can be defined for the pyramids. Before defining this density function, the list of attributes will be denoted as $\mathbf{f}$; writing $\mathbf{f}$ for ($\underline{p}$, $\underline{q}$, $\underline{h}$, H_V, $\dot{H}_V$) results in a shorter notation and simplification in formulas. The physical concept of $\mathbf{f}$ is that it identifies a particular class of pyramids; and in a unit spatial volume of fragments about a spatial point $\underline{x}$, it is meaningful to count the number of pyramids with the attribute value $\mathbf{f}$. This unit spatial volume can be taken as the volume of fragmented pellets in a spent fuel rod, or for purposes of analyzing dissolution tests, the volume of fragments used in the testing apparatus. Furthermore, since this number of pyramids may change over time as

dissolution progresses (for example, the small ones may disappear), it is necessary to also consider the value of time at which the number of pyramids are counted. With this definition for an attribute variable and the remarks on the number of pyramids, a physical definition for a pyramidal density function is as follows: let the density function $F(\underline{x}, \tau, f)$ denote the probable number of pyramids at spatial point $\underline{x}$, time τ, and attribute value f per unit spatial volume per unit attribute volume. The function F can be of discrete, countable histogram and/or continuous form. For later purposes of integration over argument variables in the density function F the spatial domain of $\underline{x}$ values is a volume space B and the attribute domain of f values is an attribute space {f}. Using the notation just defined, the density function F, and equation (1), a probabilistic dissolution rate for radionuclide species "K" in a spatial volume $d\underline{x}$ about point $\underline{x}$ and in an attribute volume df about attribute value f at time τ is written as

$$\dot{D}_{VK}(\underline{x}, \tau, f)\, df\, d\underline{x} = I_{VK}\, h_i\, e_{ijk}\, p_j q_k\, (1-H_V)^2\, \dot{H}_V\, F(\underline{x}, \tau, f)\, df\, d\underline{x} \qquad (2)$$

where the differences between grain boundary and grain volume dissolution rates and inventories within a fragment are neglected. Equation (2) is idealistic, but it is believed worthwhile to consider the consequences of an ideal experiment in which fragments were all the same (spatially homogeneous) size and shape, and thus, the pyramids would all be the same height. Assume that the dissolution velocity $\dot{H}_V h$ is spatially uniform and constant in the volume B. Then, for a set of pyramids held stationary in volume B, the time evolution of the density function F depends only on the attribute variable H_V which is the integral over time of $\dot{H}_V$. In this case the dissolution rate response, when integrated over spatial volume B and attribute space {f} can be written as

$$\dot{D}_{VK}(\tau) = \int_B \int_{\{f\}} I_{VK}\, h_i\, e_{ijk}\, p_j q_k\, (1-H_V)^2\, \dot{H}_V\, F(\underline{x}, \tau, f)\, df\, d\underline{x}$$

$$= 3I_{VK}\,\bar{P}\,\bar{F}_B\,(1 - \dot{H}_V\tau)^2\,\dot{H}_V \quad \text{for } 0 < \tau < 1/\dot{H}_V \qquad (3)$$

where $\bar{P} = h_i\, e_{ijk}\, p_j q_k/3$ is the average pyramidal volume, $\bar{F}_B$ is the number of pyramids in spatial volume B, $\dot{H}_V\tau$ is the value of H_V at time τ, and at $\tau = 1/\dot{H}_V$ dissolution of the fragments is completed. Equation (3) shows that for everything idealized, the geometric surface effect on dissolution rate response is quadratic in time and that it spans a finite time domain that depends on the fragment size and the material removal velocity. For sample sets of fragments of equal initial mass, each uniform in shape and spatially homogeneous, the set with the small sized fragments will have the largest initial surface area; and according to equation (3) the highest sample dissolution rate response over the shortest time interval. Although equation (3) is an idealized case, equation (3) can be applied for some special cases where grain boundary effects are neglectable; for example, the inventory of a radionuclide in the grain boundary is neglectably small or the dissolution rate of the grain boundary is the same as the grain volume for a radionuclide with a spatially uniform inventory.

However, there exist some cases where the grain boundary inventories of radionuclides are believed to be concentrated and where the grain boundary dissolution rates may be larger than the adjacent grain volumes. In order to represent these influences of grains on dissolution, consider a brief review, along with some minor modifications, to the description of grain boundary/volume statistics discussed in reference [4]. In reference [4], the individual grains were subdivided into pyramidal volumes analogously to the previous discussion for fragments. For grains, the exterior surface of each grain was approximated by planes; and each plane was described by two orthogonal vectors, $\underline{a}$ and $\underline{b}$, such that their cross product vector gave an effective measure of the area and orientation of the plane. These planes became base planes for a pyramidal decomposition of the grain volume, the height of the pyramid was a vector $\underline{c}$ from the base phase to the center of the

grain; and $\underline{c}$ was parallel to the cross product vector of $\underline{a} \times \underline{b}$. Thus, pyramidal subvolumes of grains, with physical attributes of ($\underline{a}$, $\underline{b}$, $\underline{c}$) are analogs of fragment pyramids whose physical attributes are ($\underline{p}$, $\underline{q}$, $\underline{h}$); only the size of grain pyramids are typically orders of magnitude less than fragment pyramids. Because of this, the analysis that follows has "two length scales" involved. Finally, in order to represent vectorially the material volume contribution for a radionuclide from grain boundary dissolution, the width of a grain boundary is divided by two and the halves are assigned separately to the pyramidal subvolume of their adjacent grain. Thus, half-widths of $w\underline{c}$ are the vector dimensions assigned to a grain boundary. In terms of Cartesian tensor notation, the volume of a single grain boundary between two adjacent grains is $2wc_i\, e_{ijk}\, a_j\, b_k$.

In a unit volume of a fragment there will be large number of grain boundaries whose combined volumes (exposed to dissolution) must be represented. Thus, a density function for the number of grain boundaries, or grain pyramids, will be a useful function and is an analog to that given for the pyramid density of fragments. The attribute variables for a grain boundary are ($\underline{a}$, $\underline{b}$, $\underline{c}$, w); which for shorthand notation will be denoted as g. Then, just as for fragments, the spatial coordinate $\underline{x}$ and a time value τ are added to define a grain boundary density function G ($\underline{x}$, τ, g). The value of G at a spatial point $\underline{x}$, a time τ, and attribute value g gives the probable number of grain boundaries per unit spatial volume per unit attribute volume of g. In the case of the grain boundary density function, G, the *spatial domain of* $\underline{x}$ *is within a pyramidal spatial domain from the set of fragments*, and it will be addressed in the following. The grain attribute domain for variable g will be denoted as {g}.

In order to separate the contributions from grain boundaries and grain volumes to dissolution rate for a radionuclide species "K", the inventories in a grain boundary for the "K^{th}" radionuclide will be denoted as I_{BK} and the inventory in a grain volume for the "K^{th}"

radionuclide will be denoted with I_{VK} as used previously. Now, the dissolution of a fragment surface, when decomposed into pyramidal basal planes, will expose an area of grain volumes and an area of grain boundaries. The sum of these two areas is the total area of the basal plane. The basal plane area without the grain boundary area at time τ was represented previously in equation (1). This leaves a representation for the exposed grain boundary area to be developed. To develop this expression imagine a straight line parallel to vector $\underline{p}$ on an exposed basal plane; this line will intersect a number of grain boundaries. Each grain boundary that is intersected will have two half thicknesses, each in vector form is $w\underline{c}$, and each is directed into the adjacent grain volume. The addition of the $w\underline{c}$ thicknesses of all grain boundaries that the straight line intersects gives a vector measure of the total grain boundary thickness in a direction parallel to vector $\underline{p}$. This vector of grain boundary thicknesses is given by the following line integral over a $\underline{p}^*$ vector length on the fragment surface

$$X_m(\underline{p}^*) = \int_{\{g\}} \int_0^{\underline{p}^*} wc_m \, e_{ijk} \, a_j \, b_k \, G(\underline{x}, \tau, g) \, dx_i \, dg \qquad (4)$$

Similarly, in the $\underline{q}$ direction of the basal plane the vector of grain boundary thicknesses over a $\underline{q}^*$ vector length can be written as

$$X_n(\underline{q}^*) = \int_{\{g\}} \int_0^{\underline{q}^*} wc_n \, e_{ijk} \, a_j \, b_k \, G(\underline{x}, \tau, g) \, dx_i \, dg \qquad (5)$$

Physically, equations (4) and (5) provide the probable thickness for the number of grain boundaries with widths $w_{\underline{\ell}}$ that the dx_i line intersected in spatial volume elements of $e_{ijk}\, a_j\, b_k\, dx_i$ along lines (0 to $\underline{p}^*$) and (0 to $\underline{q}^*$) when their number density $G(\underline{x}, \tau, g)$ is known per unit volume. Since this is the accumulated thickness of all grain boundaries, the cross product of vectors $X_m(\underline{p}^*)$ and $X_n(\underline{q}^*)$ with their orthogonal vectors $\underline{q}^*$ and $\underline{p}^*$, respectively, give the areas for edges of grain boundaries exposed on a basal plane of a dissolving pyramid. In Cartesian tensor notation this probable area is expressed by two separate terms as

$$A_\ell(\underline{X}, \underline{q}^*) = e_{\ell mn}\, X_m\, (\underline{p}^*)\, q^*_n \qquad (6a)$$

$$A_\ell\, (\underline{p}, \underline{X}) = e_{\ell mn}\, p^*_m\, X_n\, (\underline{q}^*) \qquad (6b)$$

The first gives the area from the integrated (summed) grain boundary thickness in the $\underline{p}$ direction crossed into the $\underline{q}$ direction; and the second gives the area from the integrated (summed) grain boundary thickness in the $\underline{q}$ direction crossed into the $\underline{p}$ direction; both are on the basal plane of a pyramid.

In addition to these two areas, there also exist the probability of a grain boundary plane oriented such that its normal is parallel to the pyramidal height direction $\underline{h}$; in this case the area contributions to equations (6a) and (6b) would be zero. However, this grain boundary areal contribution to the pyramidal surface exists during dissolution and can be represented by an integration along the pyramidal height vector $\underline{h}$. This is an accumulation of probable grain boundary thicknesses at a point on the pyramidal base plane as the dissolution front propagates in the height direction $\underline{h}$, thus

$$X_j(\underline{h}^*) = \int_{\{g\}} \int_0^{\underline{h}^*} wc_j\, e_{mkl}\, a_k\, b_l\, G(\underline{x}, \tau, g)\, dx_m\, dg \qquad (7)$$

The total probable grain boundary thickness from exposed boundary edges on the basal planes of pyramids in equations (4) and (5) can be approximated by the mean value theorem of integral calculus to remove the "small length scale" and obtain

$$X_m(\underline{p}^*) = \int_{\{g\}} wc_m\, e_{ijk}\, a_j\, b_k\, p^*_i\, G dg \qquad (8a)$$

$$X_n(\underline{q}^*) = \int_{\{g\}} wc_n\, e_{ijk}\, a_j\, b_k\, q^*_i\, G dg \qquad (8b)$$

Combining equations (6) and (8), the two contributions to edge areas of grain boundaries exposed on the basal pyramidal planes for dissolution are

$$A_\ell(\underline{X}, \underline{q}^*) = \int_{\{g\}} e_{\ell mn}\, wc_m\, e_{ijk}\, a_j\, b_k\, p^*_i\, q^*_n\, G dg \qquad (9a)$$

$$A_\ell(\underline{X}, \underline{p}^*) = \int_{\{g\}} e_{\ell mn}\, wc_n\, e_{ijk}\, a_j\, b_k\, q^*_i\, p^*_m\, G dg \qquad (9b)$$

Finally, the other area of grain boundary surfaces exposed per unit length $\underline{h}^*$ in the $\underline{h}$ direction over the total area of the base plane ($\underline{p}^* \times \underline{q}^*$) of a pyramid is defined from equation (7)

$$A_m(\underline{X}, \underline{h}^*) = \int_{\{\underline{g}\}} wc_j \, e_{mk\ell} \, a_k \, b_\ell \, e_{jin} \, p^*_i \, q^*_n \, G d\underline{g} \qquad (9c)$$

The sum over equations (9) gives the total probable area of grain boundary exposed on a pyramidal base plane whose nominal areal dimensions are given by ($\underline{p}^*$, $\underline{q}^*$). Then, given that the dissolution rate of grain boundaries in the pyramidal height direction $\underline{h}$ is at a velocity of $\dot{H}_B\underline{h}$, the probable volume rate of grain boundary material removed by all three areal contributions of equations (9) is

$$\dot{V}_B = A_\ell (\underline{X}, \underline{q}^*) \, \dot{H}_B \, h_\ell + A_\ell (\underline{X}, \underline{p}^*) \, \dot{H}_B \, h_\ell + A_m (\underline{X}, \underline{h}^*) \, \dot{H}_B \, h_m \qquad (10)$$

Using equation (10), the dissolution rate for radionuclide species K from grain boundaries is given for a single pyramid of attribute value $\mathbf{f}$ by

$$\dot{D}^{\epsilon}_{BK} (\tau) = I_{BK} \, \dot{V}_B \qquad (11)$$

where I_{BK} is the grain boundary inventory of radionuclide species K per unit grain boundary volume. Equation (11) can be used to find the grain boundary dissolution rate for a set of fragments by summing over the probable number of pyramids of the fragment set. Thus, for the number of pyramids given by $F \, df \, d\underline{x}$, equation (11) for τ near zero becomes

$$\dot{D}_{BK} (x, \tau, \mathbf{f}) \, df \, d\underline{x} = I_{BK} \, \dot{V}_B \, F(\underline{x}, \tau, \mathbf{f}) \, df \, d\underline{x} \qquad (12)$$

where the attribute variables of $\mathbf{f}$ must be extended to contain $\dot{H}_B$ also.

An expression can now be written for the early time (τ near zero before the formation of a zone of dissolution illustrated in Figure 1) dissolution rate response from both grain boundaries and grain volumes. Recall that equation (2) was for a surface at some arbitrary time τ, but at early times $(1-\dot{H}_V\tau)^2$ is essentially 1, then the exposed grain volume area is the initial pyramidal base plane (i.e., $\underline{p} \times \underline{q}$) minus the exposed grain boundary areas given in equations (9). For t near zero, the grain boundary areas of equations (9) are evaluated on the initial pyramidal base plane; thus, $\underline{p}^*$ is equal to $\underline{p}^*$ and $\underline{q}^*$ is equal to $\underline{q}$. Then, the reduction of surface area due to exposed grain boundary area can be easily made by writing the grain boundary volume removal rate as a velocity relative to the surface $\dot{H}_V\underline{h}$. Thus, the $\dot{H}_B\underline{h}$ of equation (10) would be replaced with $(\dot{H}_B - \dot{H}_V)\underline{h}$. Making this change in equations (2), (11) and (12) is the easiest way of expressing the combined contributions; which for early times and for radionuclide species K is

$$\dot{D}_K(\underline{x}, \tau, f)\, df\, d\underline{x} = I_{VK}\, h_i\, e_{ijk}\, p_j\, q_k\, \dot{H}_V\, F(\underline{x}, \tau, f)\, df\, d\underline{x}$$

$$+ (I_{BK}\dot{H}_B - I_{VK}\dot{H}_V) \int_{(g)} (e_{\ell mn}\, wc_m\, e_{ijk}\, a_j\, b_k\, p_i\, q_n\, h_\ell + e_{\ell mn}\, wc_n\, e_{ijk}\, a_j\, b_k\, q_i\, p_m\, h_\ell$$

$$+ e_{jin}\, wc_j\, e_{mk\ell}\, a_k\, b_\ell\, p_i\, q_n\, h_m)\, G(\underline{x}, \tau, g)\, dg\, F(\underline{x}, \tau, f)\, df\, d\underline{x} \qquad (13)$$

Equation (13) describes an early time dissolution process where the grain volume surface areas with their inventory I_{VK} are dissolving along vector $\underline{h}$ at a rate $\dot{H}_V\underline{h}$ and the grain boundary surface areas with their inventories I_{BK} are dissolving at a rate $\dot{H}_B\underline{h}$. Note however, that the two grain boundary terms with exposed edges are dissolving at a rate

$\dot{H}_{Bh}$ and removing a grain boundary width w_g of material adjacent to each grain. These are to be compared with the last grain boundary term, which represents the effective dissolution of grain boundary planes whose normals are parallel to the height vector $\underline{h}$ of the pyramid. For times near $\tau = 0$, these planes would be near the initial base plane ($H_V = 0$) of a pyramid. However, for later times, and assuming that $\dot{H}_{Bh}$ is greater than $\dot{H}_{Vh}$, these planes would reside interior to a pyramidal volume of height $h(1-H_V)$. This evolves into a zone of dissolution illustrated in Figure 1. Thus, there would be two dissolution fronts, one on exterior pyramidal grain surfaces propagating at $\dot{H}_{Vh}$ and one interior to the pyramidal subvolume that dissolves grain boundaries as it propagates along vector $\underline{h}$ at $\dot{H}_{Bh}$ and also dissolves lateral grain boundary planes (those with thickness direction normals along $\underline{h}$) in passing. Thus, after a period of time, equation (13) would not describe the dependence of dissolution rate on the positions of the two dissolution fronts and their current sizes (i.e., $\underline{p}^* \times \underline{q}^*$).

Equation (13) can be extended such that the assumption of τ near zero no longer need apply; however, other assumptions are required. The other assumptions are necessary to describe whether or not the exterior grains fall off as the grain boundaries dissolve along $\underline{h}$ over distances greater than the dimensions of the grains and whether the width of the grain boundary w_g continues to increase in time as the time increases. For purposes of this preliminary modelling, it will be assumed that grains do not fall off and that the grain boundaries have a single dissolved width w_g as the grain boundary dissolution front propagates into the fragment pyramidal volume. The first assumption is proposed as reasonable for unoxidized UO_2 spent fuel because some few undissolved material ligaments on lateral grain boundaries would be sufficient to hold grains to fragments. The second assumption is made primarily to simplify the model development that follows. Alternative assumptions to both of these can be made and dissolution rate

expressions derived; however, these two are proposed as conditions on the preliminary model developed in this paper.

The above describes a two front dissolution problem, one front is on grain volume surfaces at position $H_V\underline{h}$ along $\underline{h}$ and the other front is on grain boundary surfaces at position $H_B\underline{h}$ along $\underline{h}$, where H_B is the time integral of $\dot{H}_B$. Thus, the attribute variables of f must be extended to contain both $\dot{H}_B$ and H_B for this latter case. Now for grain boundary dissolution at constant width $w\underline{c}$, the grain volume surfaces that are between the pyramidal base plane at $H_V\underline{h}$ and $H_B\underline{h}$ have already dissolved as the grain boundary dissolution front propagates past them. Thus, only the exposed grain volume surfaces that coincide with the pyramidal fragment base plane located at $H_V\underline{h}$ are dissolving; and their rate of dissolution is along vector $\underline{h}$ at a propagation rate of $\dot{H}_V\underline{h}$. Using the assumptions and their consequences discussed above, the form of equation (13) can be modified for the long time dissolution rate response. First, the area of the grain volume dissolution front is to be modified with the factor $(1\text{-}H_V)^2$ to account for the decreased length in vectors $\underline{p}$ and $\underline{q}$ at position $H_V\underline{h}$ along the height vector. This area is further reduced by subtracting the area of the exposed grain boundary edges and the lateral plane grain boundary areas which were dissolved, except for a few ligaments, as the grain boundary dissolution front propagated into the pyramid. Secondly, the area at the grain boundary dissolution front is reduced by the factor of $(1\text{-}H_B)^2$ to account for the decreased length in vectors $\underline{p}$ and $\underline{q}$ at position $H_B\underline{h}$ along the height vector. Making these modifications to equation (13), the dissolution rate for a number of pyramids Fdfd$\underline{x}$ is rewritten as

$$\dot{D}_K(\underline{x}, \tau, f)\, df\, d\underline{x} = I_{VK}\, \dot{H}_V \{h_\ell\, e_{\ell jk}\, p_j q_k - \int_{\{g\}} (h_\ell\, e_{\ell mn}\, wc_m\, e_{ijk}\, a_j\, b_k\, p_i\, q_n$$

$$+ h_\ell\, e_{imn}\, wc_n\, e_{\ell jk}\, a_j\, b_k\, q_i\, p_m$$

$$+h_\ell\, e_{\ell mn}\, wc_n\, e_{ijk}\, a_j\, b_k\, q_i\, p_m)\, G(\underline{x}, \tau, g)\, dg_j\, (1-\bar{H}_V)^2\, F(\underline{x}, \tau, \bar{f})\, df\, d\underline{x} +$$

$$I_{BK}\, \dot{H}_B \int_{\{\underline{g}\}} (e_{\ell mn}\, wc_m\, e_{ijk}\, a_j\, b_k\, p_i\, q_n\, h_\ell + e_{\ell mn}\, wc_n\, e_{ijk}\, a_j\, b_k\, q_i\, p_m\, h_\ell$$

$$+ e_{jin}\, wc_j\, e_{\ell km}\, a_k\, b_m\, p_i\, q_n\, h_\ell)\, G\,(\underline{x}, \tau, g)\, dg\, (1-H_B)^2\, F(\underline{x}, \tau, f)\, df\, d\underline{x} \qquad (14)$$

Equation (14) was derived based on two assumptions; one was that exterior surface grains do not fall off and the other was that the width $w_{\underline{c}}$ of grain boundary dissolution was a constant and the same value everywhere in the set of pyramids. Although equation (14) has many terms, it can be observed that when the magnitude of the grain boundary dissolution width $|w_{\underline{c}}|$ is small compared to the grain sizes dimensions $|\underline{c}|$, and $|\underline{a}|$ and $|\underline{b}|$, the volume of the dissolved grain boundary material will be small compared to the pyramidal volume. Thus, for the dissolved grain boundary volume to influence the overall dissolution rate, the product of dissolution rate $\dot{H}_B$ and the inventory I_{BK} of the grain boundaries must be very large. These conditions may possibly exist for some high burnup fuels, since it is believed that the more soluble radionuclide species migrate to and are trapped in grain boundaries [1,6]. However, additional dissolution testing is necessary to provide both data and an understanding of the dissolution rate response of spent fuel. At this point, the above dissolution rate equation is available that incorporates both a grain volume dissolution front and a grain boundary dissolution front, both of which can propagate at different velocities. It will be necessary to perform additional experiments to determine these velocities. However, from relatively short term experiments, an upper

bound estimate on these velocities may be possible and the effects of grain boundary dissolution rates be assessed for those radionuclides which are believed to be concentrated at grain boundaries. Nonetheless, for the ideal case of uniform fragments dissolving at constant rates $\dot{H}_V$ and $\dot{H}_B$, Equation (14) predicts that the grain boundary dissolution rate contribution in a fragment decreases as $(1-\dot{H}_B\tau)^2$ in time and the grain volume contribution for a fragment decreases as $(1-\dot{H}_V\tau)^2$.

Physically, the first term on the right hand side of equation (14) represents the dissolution rate on an exterior surface of exposed grain volume area minus the area from previously dissolved grain boundary edges that intersect this exterior surface; and the second term represents the dissolution rate on an interior surface front of all grain boundary volumes (grain boundary areas with width w_ξ). The exterior surface dissolution front is propagating at a material removal rate $I_{VK}\,\dot{H}_V h_\ell$. The interior surface dissolution front is propagating at a material removal rate $I_{BK}\,\dot{H}_B h_\ell$. The position of the interior front relative to the exterior front is $(H_B - H_V)h$ at any time τ where H_B and H_V are the integrals over time of $\dot{H}_B$ and $\dot{H}_V$, respectively. The material between $H_B h$ and $H_V h$ was illustrated as a zone of dissolution in Figure 1. If this zone of dissolution becomes constant in thickness after some transient period of time, then the rates $\dot{H}_B$ and $\dot{H}_V$ become equal also. Physically, one would expect that a finite transient time interval exists and that $\dot{H}_B$ approaches $\dot{H}_V$; because the transport of dissolved material from the interior surface front outward to the exterior surface front becomes exceedingly more difficult in the narrow and tortuous pathways that increasingly extend into a fragment along the dissolving grain boundaries.

This leads to a conjecture that even if $\dot{H}_B$ is initially much larger than $\dot{H}_V$, within a few grain size lengths it would be reduced. A simple phenomenological time response for $\dot{H}_B$ can be developed from a linear diffusion process to give $\dot{H}_B(\tau) = (\dot{H}_{BO} + \dot{H}_{BO}\tau)^{-1/2}$;

where $\dot{H}_B$ and $\dot{H}_{BO}$ are both constants. This form of $\dot{H}_B$ is monotonically decreasing in time. However, when $\dot{H}_B$ becomes equal to $\dot{H}_V$, then physically, it should remain equal to $\dot{H}_V$ thereafter; assuming that all other environmental conditions remain the same. While this is a physically reasonable conjecture, experiments are necessary to test it. Certainly, one may find that this conjecture is not supported merely because grains on the exterior surface fall off as the interior front propagates into a fragment. Future experiments will thus determine the directions of future model developments. However, this preliminary model development can be used to plan future experiments and the quantitites that need to be measured in those experiments.

Finally, the previous expressions for dissolution rate response from exposed grain volume and grain boundary areas of spent fuel fragments did not explicitly address an initial dissolution "pulse" rate of the volatile radionuclides that are transported out of the UO_2 fragments during reactor operation to the cladding-fragment surfaces [1]. These volatile radionuclides are believed to form a concentrated layer on fragment surfaces. In this case, the heterogeneity of this layer can be represented in the dissolution rate expressions by generalizing the inventory term I_{VK}. In this generalization, the inventory I_{VK} could be represented as a function of H_V to describe the concentration and layer thickness of the volatile radionuclides that reside on the surfaces of spent fuel fragments.

SUMMARY

The dissolution rate response of spent fuel radionuclides can depend on the dissolution rates over grain volume surfaces and over grain boundary surfaces for a set of fragments. Since fragments are geometrically somewhat arbitrary in size and shape, plus the interior characteristics of grain boundary/volume geometries are not readily described in

a deterministic sense, statistical concepts were applied to describe both fragments and grains within a fragment. This approach results in a "two length scale" problem; one length scale is a measure of fragment size from broken spent fuel pellets, and the other length scale is a measure of grain size in fragments of spent fuel. With this approach, a preliminary dissolution rate model was developed that consisted of expressions describing the dissolution rate from the radionuclide inventory on exposed grain volume surface times the intrinsic material removal rate of grain volumes plus the dissolution rate from radionuclide inventory on exposed grain boundary surface times the intrinsic material removal rate of grain boundaries. In the near future, the equations of this dissolution rate model will be used to analyze further the data obtained from specially designed grain-sized dissolution tests [7]. For these tests, the grain-sized particles, with their associated grain boundaries, are produced by crushing spent fuel fragments; the fracture planes of the crushed fragments are primarily the grain boundary planes. The purposes of these tests are to measure grain boundary inventory heterogeneity and the long term "matrix" (grain volume) dissolution rate. In addition to this application, this preliminary model for dissolution rate will be used to plan additional spent fuel dissolution tests and to assess the potential of the tests to isolate the influence of inventory, surface area, and intrinsic material removal rate. In this way, a mechanistic understanding of the dissolution process will be attained.

ACKNOWLEDGEMENT

The authors wish to thank Miss T. Fletcher for the excellent organization and timely typing of this paper. Work performed under the auspices of the U.S. Dept. of Energy, Office of Civilian Radioactive Waste Management, Yucca Mountain Project, by the Lawrence Livermore National Laboratory under contract number W-7405-ENG-48.

REFERENCES

1. Johnson, L. H., and D. W. Showsmith, Spent Fuel, Chapter 11, published in Radioactive Waste Forms for the Future, editors W. Lutze and R. C. Ewing, pp. 635-698, North Holland Physics Publishing, Elsevier Sc. Pub., 1988.

2. Wilson, C. N., Results from NNWSI Series 2 Bare Fuel Dissolution Tests, Battelle-Pacific Northwest Laboratory Report PNL-7169, September 1990.

3. Wilson, C. N., Results from NNWSI Series 3 Spent Fuel Dissolution Tests, Battelle-Pacific Northwest Laboratory Report PNL-7170, June 1990.

4. Stout, R. B., H. F. Shaw, and R. E. Einziger, Statistical Model for Grain Boundary and Grain Volume Oxidation Kinetics in UO_2 Spent Fuel, Lawrence Livermore National Laboratory Report UCRL-100859, September 1989.

5. Stout, R. B., Statistical Model for Particle-Void Deformation Kinetics in Granular Materials during Shock Wave Propagation, Lawrence Livermore National Laboratory Report UCRL-101623, July 1989.

6. Guenther, R. J., D. E. Blahnik, L. E. Thomas, D. L. Baldwin, and J. E. Mendel, Radionuclide Distribution in LWR Spent Fuel, Battelle-Pacific Northwest Laboratory Report PNL-SA-18168, May 1990.

7. Gray, W. J., and D. M. Strachan, UO_2 Matrix Dissolution Rates and Grain Boundary Inventories of Cs, Sr, and Tc in Spent LWR Fuel, Battelle-Pacific Northwest Laboratory Report PNL-SA-18268, May 1990.

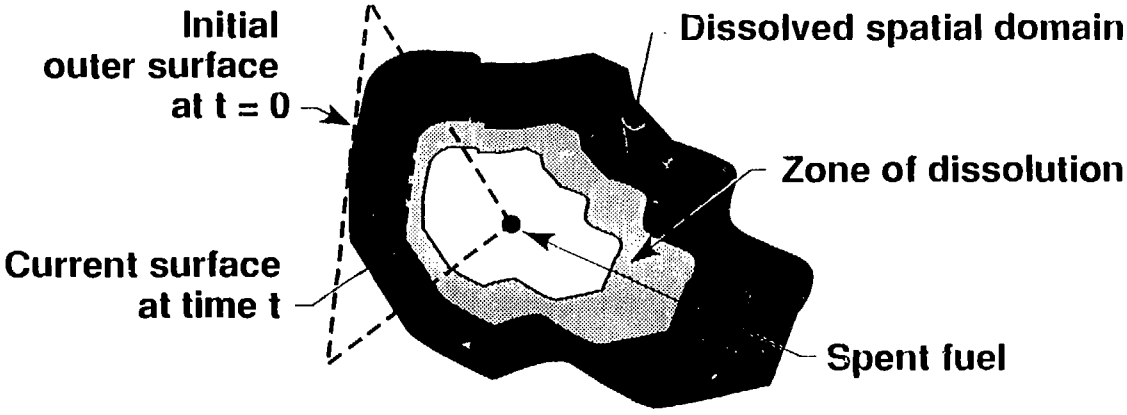

Figure 1. Illustration of a dissolving fragment